# S

## Scaling and Scale Invariance

S. Lovejoy
Physics, McGill University, Montreal, Canada

### Definition

Scaling is a scale symmetry that relates small and large scales of a system in scale-free, power law manner: without a characteristic scale. Because it is a symmetry, in systems with structures/fluctuations over wide ranges of scale, it is the simplest such relationship.

In one dimension, the notion of scale is usually taken as the length of an interval, and in two or higher dimensions, the Euclidean distance is often used. However, the latter is isotropic: It is restricted to "self-similar" fractals, multifractals. Most geosystems are stratified in the vertical and have other anisotropies so that the scale notion must be broadened. "Generalized Scale Invariance" does this with two elements: a definition of the unit scale (all the unit vectors) defining the scales of the nonunit vectors with an operator that changes scale by a given scale ratio. This scale-changing operator forms a group whose generator is a scale-invariant exponent.

Systems that are symmetric with respect to these scale changes may be geometric sets of points (fractals) or fields (multifractals). The relationship between scales is generally (but not necessarily) statistical and involves additional scaling relationships and corresponding scale-invariant exponents. These are often fractal dimensions, or codimensions (sets), or corresponding dimension, codimension functions (multifractals).

#### Scaling Sets: Fractal Dimensions and Codimensions

Geosystems typically display structures spanning huge ranges of scale in space, in time, and in space-time. The relationship between small and large, fast and slow processes is fundamental for characterizing the dynamical regimes – for example, weather, macroweather, and climate – as well as for developing corresponding mathematical and numerical models. Since scaling can be formulated as a symmetry principle, the simplest assumption about such relationships is that they are connected in a scaling manner governed by scale-invariant exponents.

In general terms, a system is scaling if there exists a "scale free" (power law) relationship (possibly deterministic, but usually statistical) between fast and slow (time) or small and large (space, space-time). If the system is a geometric set of points – such as the set of meteorological measuring stations (Lovejoy et al. 1986) – then the set is a fractal set and the number of points $n$ in a circle radius $L$ varies as:

$$n(L) \propto L^D \tag{1}$$

where the (scale invariant) exponent $D$ is the fractal dimension (Mandelbrot 1977). Consider instead, the density of points $\rho(L)$:

$$\rho(L) \propto n(L)/L^d \approx L^{-c}; \quad c = d - D \tag{2}$$

where $d$ is the dimension of space (in this example, stations on the surface of the Earth, $d = 2$ and empirically, $D \approx 1.75$). The exponent of ρ characterizes the sparseness of the set; its exponent $c$ is its fractal *codimension*. For geometric sets of points, it is the difference between the dimension of the embedding space and the fractal dimension of the set. More generally, codimensions characterize probabilities and therefore statistics; they are usually more useful than fractal dimensions (see below). The distinction is important for considering stochastic processes that are typically defined on infinite dimensional probability spaces so that $d, D \to \infty$ even though $c$ remains finite. Notice that whereas $n(L)$ and $\rho(L)$ are scaling, their exponents $D$ *and* $c$ are scale invariant; the two notions are closely linked.


B. S. Daya Sagar et al. (eds.), *Encyclopedia of Mathematical Geosciences*, Encyclopedia of Earth Sciences Series,
https://doi.org/10.1007/978-3-030-26050-7_282-1

### Scaling Functions, Fluctuations, and the Fluctuation Exponent *H*

Geophysically interesting systems are typically not sets of points but rather scaling fields such as the rock density or temperature $f(\underline{r}, t)$ at the space-time point $(\underline{r}, t)$. (We will generally use the term "scaling fields," but for multifractals, the more precise notion is of singular densities of multifractal measures). In such a system, some aspect – most often a suitably defined fluctuation – $\Delta f$ – has statistics whose small and large scales are related by a scale-changing operation that involves only the scale ratios: Over the scaling range, the system has no characteristic size.

In one dimension – temporal series $f(t)$ or spatial transects, $f(x)$ – scaling can be expressed as:

$$\Delta f(\Delta t) \stackrel{d}{=} \varphi_{\Delta t} \Delta t^H \tag{3}$$

where $\Delta f$ is a fluctuation, $\Delta t$ is the time interval over which the fluctuation occurs, $H$ is the fluctuation exponent, and $\varphi_{\Delta t}$ is a random variable that itself generally depends on the scale (for transects, replace $\Delta t$ by the spatial interval $\Delta x$). The sign $\stackrel{d}{=}$ is in the sense of random variables; this means that the random fluctuation $\Delta f(\Delta t)$ has the same probability distribution as the random variable $\varphi_{\Delta t} \Delta t^H$. In one dimension, the notion of scale can be taken to be the absolute temporal or spatial interval $\Delta t$, $\Delta x$; for processes in two or higher dimensional spaces, the definition of scale itself is nontrivial and we need Generalized Scale Invariance (GSI) discussed later.

Although the general framework for defining fluctuations is wavelets, the most familiar fluctuations are either $\Delta f(\Delta t)$ taken as a scale $\Delta t$ difference: $\Delta f(\Delta t) = f(t) - f(t - \Delta t)$, or a scale $\Delta t$ anomaly $f'_{\Delta t}$ which is the average over the interval $\Delta t$ of the series $f' = f - \overline{f}$ whose overall mean $\overline{f}$ has been removed. We suppress the $t$ dependence of $\Delta f$ since we consider the case where the statistics are independent of time or space: They are respectively statistically stationarity or statistically homogeneous. Physically, this is the assumption that the underlying physical processes are the same at all times and everywhere in space. Difference fluctuations are typically useful when average fluctuations increase with scale ($1 > H > 0$), whereas anomaly fluctuations are useful when they decrease with scale $-1 < H < 0$. A simple type of fluctuation that covers both ranges (i. e., $-1 < H < 1$) is the Haar fluctuation (Lovejoy and Schertzer 2012) that appears to be adequate for almost all geoprocesses.

To see that fluctuations obey the scaling property eq. 3, consider the simplest case where $\varphi$ is a random variable independent of resolution. This "simple scaling" (Lamperti 1962) is respected, for example, by regular Brownian motion in which case $H = 1/2$, $\Delta T(\Delta t)$ is a difference and $\varphi$ is a Gaussian random variable. The extensions to cases $0 < H < 1$ are called "fractional Brownian motions" (fBm, Kolmogorov 1940) and to the first differences (increments) of fBm, "fractional Gaussian noises" (fGn) with $-1 < H < 0$ (Mandelbrot and Van Ness 1968). In fGn, $\Delta f(\Delta t)$ must be taken as an anomaly fluctuation $\overline{f'}_{\Delta t}$, Haar fluctuation, or other appropriate fluctuation definition.

Although Gaussian statistics are commonly assumed, in scaling processes, they are in fact exceptional. In the more usual case, at fixed scales, the "tails" (extremes) of the probability distribution of $\varphi$ is also a power law. Scaling in probability space means that for large enough thresholds $s$, the probability of a random $\varphi$ exceeding $s$ is $Pr(\varphi > s) \approx s^{-qD}$. $q_D$ is a critical exponent since statistical moments $<\varphi^q>$ of order $q > q_D$ diverge (the notation "Pr" indicates probabiilty, "$<>$" indicates statistical averaging, and the "$D$" subscript is because the value of the critical exponent generally depends on the dimension of space over which the process is averaged). Power law probabilities (with possibly any $q_D > 0$) are a generic property of multifractal processes; more classically, they are also a property of stable Levy variables with Levy index $0 < \alpha < 2$ (for which $q_D = \alpha$; the exceptional $\alpha = 2$ case is the Gaussian, all of whose moments converge so that $q_D = \infty$). Probability distributions with power law extremes can give rise to events that are far larger than those predicted from Gaussian models, indeed they can be so strong that they have sometimes been termed "black swans" (Adapted from Taleb 2010 who originally termed such extreme events "grey swans"). Empirical values of $q_D$ in the range 3–7 for geofields ranging from the wind, precipitation, temperature, and seismicity have been reported in dozens of papers, (many are reviewed in ch.5 of Lovejoy and Schertzer 2013 that also includes the theory).

To see why Eq. 3 has the scaling property, consider the simplest case where the fluctuations in a temporal series $f(t)$ follow eq. 1, but with $\varphi$ a random variable independent of resolution: $\varphi_{\Delta t} \stackrel{d}{=} \varphi$. If we denote $\lambda > 1$ as a scale ratio, it is easy to see that the statistics of large-scale ($\Delta f(\lambda \Delta t)$) and small-scale ($\Delta f(\Delta t)$) fluctuations are related by a power law:

$$\Delta f(\lambda \Delta t) \stackrel{d}{=} \lambda^H \Delta f(\Delta t) \tag{4}$$

Equation 4 directly shows the scaling property relating the fluctuations differing by a scale ratio $\lambda$. Since the scaling exponent $H$ is the same at all scales, it is scale invariant.

Here and below, we treat time series and spatial sections (transects) without distinction, their scales are simply absolute differences in time $\Delta t$, or in space $\Delta x$. This ignores the sometimes important difference that – due to causality – the sign of $\Delta t$ (i.e., whether the interval is forward or backward in time) can be important; whereas in space one usually assumes left-right symmetry (the sign of $\Delta x$ is not important), here we treat both as absolute intervals (see Marsan et al. 1996).

Equation 4 relates the probabilities of small and large fluctuations; it is usually easier to deal with the deterministic equalities that follow by taking $q^{th}$ order statistical moments of Eq. 3 and then averaging over a statistical ensemble (indicated by "< >"):

$$\langle(\Delta f(\Delta t))^q\rangle = \langle \varphi_{\Delta t}^q \rangle \Delta t^{qH} \tag{5}$$

The equality is now a usual, deterministic one. Eq. 5 is the general case where the resolution $\Delta t$ is important for the statistics of $\varphi$. In general, $\varphi_{\Delta t}$ is a random function or field averaged at resolution $\Delta t$; if it is scaling, its statistics will follow:

$$\langle \varphi_\lambda^q \rangle = \lambda^{K(q)}; \quad \lambda = \tau/\Delta t \geq 1 \tag{6}$$

where $\tau$ is the "outer" (largest) scale of the scaling regime satisfied by the equation, and $\lambda$ is a convenient dimensionless scale ratio. $K(q)$ is a convex ($K''(q) \geq 0$) exponent function; since the mean fluctuation is independent of scale ($\langle \varphi_\lambda \rangle = \lambda^{K(1)} = const$), we have $K(1) = 0$.

Equation 6 describes the statistical behavior of cascade processes; these are the generic multifractal processes. Since large $q$ moments are dominated by large, extreme values, and small $q$ moments by common, typical values, $K(q) \neq 0$ implies a different scaling exponent for each statistical moment $q$: "multiscaling." Fluctuations of various amplitudes change scale with different exponents, and each realization of the process is a multifractal: The values that exceed fixed thresholds are fractal sets. Increasing the threshold defines sparser and sparser exceedance sets (see the "spikes" in Figs. 1a and 2); the fractal dimensions of these sets decrease as the threshold is increased; this is discussed further in the next section. In general, $K(q) \neq 0$ is associated with intermittency, a topic we treat in more detail in Sect. 2.

## Structure Functions and Spectra

Returning to the characterization of scaling series and transects via their fluctuations, we can combine eqs. 5, 6, to obtain:

$$S_q(\Delta t) = \langle(\Delta f(\Delta t))^q\rangle = \langle \varphi_{\Delta t}^q \rangle \Delta t^{qH} \propto \Delta t^{\xi(q)};$$

$$\xi(q) = qH - K(q) \tag{7}$$

where $S_q$ is the $q^{th}$ order ("generalized") structure function and $\xi(q)$ is its exponent. The structure functions are scaling since the small and large scales are related by a power law:

$$S_q(\lambda \Delta t) = \lambda^{\xi(q)} S_q(\Delta t) \tag{8}$$

When $K(q) \neq 0$, different moments change differently with scale so that, for example, the root mean square fluctuation has statistical moment $\xi(2)/2$ which can readily be smaller than the exponent of the first-order moment: $\xi(1) - \xi(2)/2 = K(2)/2 > 0$ (since $K(1) = 0$ and for all $q$, $K''(q) > 0$). This is shown graphically in Fig. 1a, b. A useful way of quantifying this deviation is the derivative at the mean: $C_1 = K'(1)$ where $C_1 \geq 0$ is the codimension of the mean fluctuation (see below). Typical values of $C_1$ are $\approx$ 0.05–0.15 for turbulent quantities (wind, temperature, humidity, and pressure (Lovejoy and Schertzer 2013) as well as topography, susceptibility, and rock density (Lovejoy and Schertzer 2007). It is significant that the Martian atmosphere has nearly identical exponents ($H$, $C_1$) to Earth (wind, temperature, and pressure,

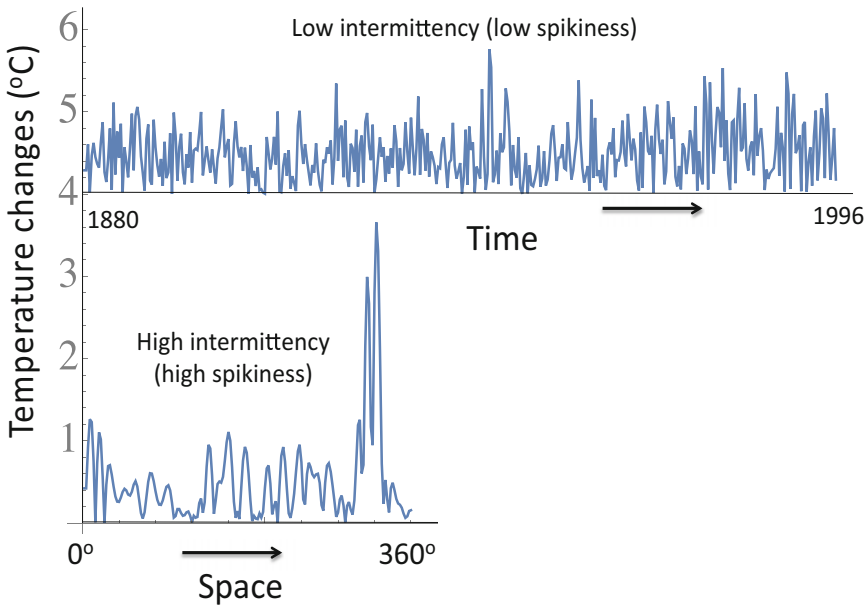


**Scaling and Scale Invariance, Fig. 1a** A comparison of temporal and spatial macroweather series at 2° resolution. The top are the absolute first differences of a temperature time series at monthly resolution (from 80° E, 10° N, 1880–1996, annual cycle removed, displaced by 4C for clarity), and the bottom is the series of absolute first differences ("spikes") of a spatial latitudinal transect (annually averaged, 1990 from 60° N) as a function of longitude. One can see that while the top is noisy, it is not very "spikey"

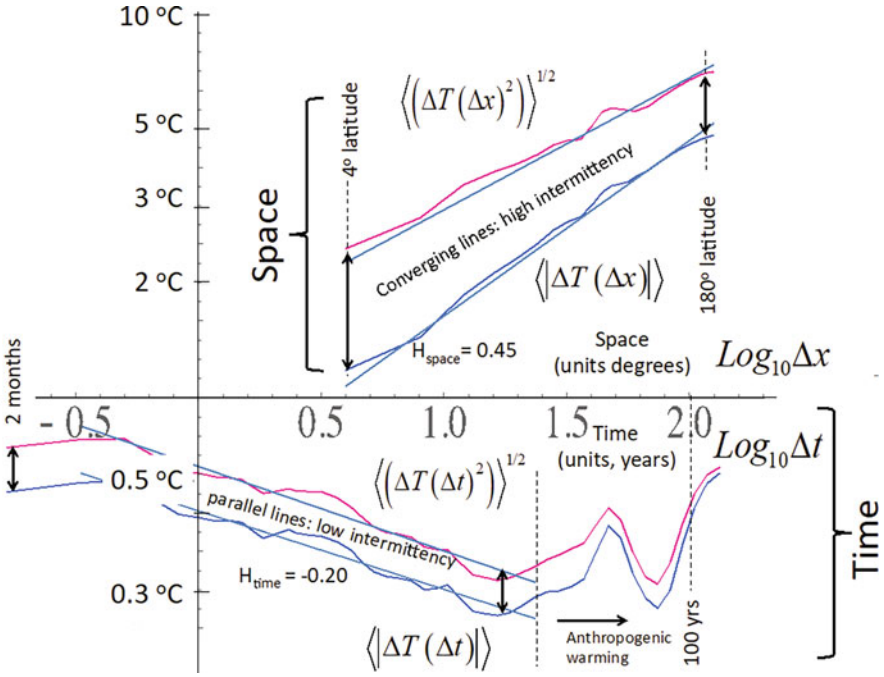


**Scaling and Scale Invariance, Fig. 1b** The first order and RMS Haar fluctuations of the series transect in Fig. 1a. One can see that in the spikey transect (space, top), the first order and RMS statistics converge at large lags ($\Delta x$), and the rate of the converge is quantified by the intermittency parameter $C_1$. The time series (bottom) is less spikey, and it converges very little and has low $C_1$ (see Fig. 1a, top). The break in the scaling at ≈ 20 years is due to the dominance of anthropogenic effects at longer time scales. Quantitatively, the intermittency parameters near the mean are $C_1 \approx 0.12$ (space), $C_1 \approx 0.01$ (time)

(Chen et al. 2016), and Martian topography is similarly close to Earth's (Landais et al. 2019).

Precipitation and seismicity are notably much more extreme with $C_1 \approx 0.4$ (Lovejoy et al. 2012), ≈1.3 (Hooge et al. 1994). We could note that whereas the moments are "scaling," the exponent functions such as $K(q)$, $\xi(q)$, etc. are "scale invariant."

Equations 7 and 8 are the statistics of (real space) fluctuations; however, it is common to analyze data with Fourier techniques. These yield the power spectrum:

$$E(\omega) \propto \left\langle \left| \widetilde{f}(\omega) \right|^2 \right\rangle \tag{9}$$

where $\widetilde{f}(\omega)$ is the Fourier Transform of $f(t)$, and $\omega$ is the frequency. Due to "Tauberian theorems" (e.g., Feller 1971), power laws in real space are transformed into power laws in Fourier space, hence for scaling processes:

$$E(\omega) \approx \omega^{-\beta} \tag{10}$$

where $\beta$ is the spectral exponent. Due to the Wiener-Khintchin theorem, the spectrum is the Fourier transform of the autocorrelation function, itself closely related to $S_2(\Delta t)$. We therefore obtain the general relation:

$$\beta = 1 + \xi(2) = 1 + 2H - K(2) \tag{11}$$

(Technical note: Scaling is generally only followed over a finite range of scales, and unless there are cut-offs, there are generally low- or high-frequency divergences. However, if the scaling holds over wide enough ranges, then scaling in real space does imply scaling of the spectrum and vice versa, and if the scaling holds over a wide enough range, then eq. 11 relates their exponents).

Returning now to the case of simple scaling, we find $\langle \varphi^q \rangle = B_q$ where $B_q$ is a constant independent of scale ($\Delta t$); hence we have $K(q) = 0$ and $S_q(\Delta t) \propto \Delta t^{qH}$ so that:

$$\xi(q) = qH \tag{12}$$

i.e., $\xi(q)$ is a linear function of $q$. This "linear scaling" with $\beta = 1 + 2H$ is also sometimes called "simple scaling." Linear scaling arises from scaling linear transformations of noises; the general linear scaling transformation is a power law filter (multiplication of the Fourier Transform by $\omega^{-H}$) which is equivalently a fractional integral ($H > 0$) or fractional derivative ($H < 0$). Fractional integrals of order $H + 1/2$ of Gaussian white noises yield fBm ($1 > H > 0$) and fGn ($-1 < H < 0$). The analogous Levy motions and noises are obtained by the filtering of independent Levy noises (in this case, $\xi(q)$ is only linear for $q < \alpha < 2$; for $q > \alpha$, the moments diverge so that both $\xi(q)$ and $S_q \rightarrow \infty$).

The more general "nonlinear scaling" case where $K(q)$ is nonzero is associated with fractional integrals or derivatives of order $H$ of scaling multiplicative (not additive) random processes (cascades, multifractals). These fractional integrals ($H > 0$) or derivatives ($H < 0$) filter the Fourier Transform of $\varphi$ by $\omega^{-H}$; this adds the extra term $qH$ in the structure function exponent: $\xi(q) = qH - K(q)$.

In the literature, the notation "$H$" is not used consistently. It was introduced in honor of Edwin Hurst a pioneer of long

memory processes sometimes called "Hurst phenomena" (Hurst 1951). Hurst introduced the rescaled range exponent notably in the study of Nile river streamflow records. To explain Hurst's findings, Mandelbrot and Van Ness [1968] developed Gaussian scaling models (fGn, fBm) and introduced the symbol "*H*." At first, this represented a "Hurst exponent," and they showed that for fGn processes, it was equal to Hurst's exponent. However, by the time of the landmark "Fractal Geometry of Nature" (Mandelbrot 1982), the usage was shifting from a scaling exponent to a model specification: the "Hurst parameter." In this new usage, the symbol $H$ was used for both fGn and its integral fBm, even though the fBm-scaling exponent is larger by one. To avoid confusion, we will call it $H_M$. Subsequently, a mathematical literature has developed using $H_M$ with $0 < H_M < 1$ to parametrize both the process (fGn) and its increments (fGn). However, also in the early 1980s (Grassberger and Procaccia 1983; Hentschel and Procaccia 1983; Schertzer and Lovejoy 1983), much more general scaling processes with an infinite hierarchy of exponents – multifractals – were discovered clearly showing that a single exponent was not enough. Schertzer and Lovejoy (1987) showed that it was nevertheless possible to keep $H$ in the role of a mean fluctuation exponent (originally termed a cascade "conservation exponent"). This is the sense of the $H$ exponent discussed here. As described above, using appropriate definitions of fluctuations (i.e., by the use of an appropriate wavelet), $H$ can take on any real value. When the definition is applied to fBm, it yields the standard fBm value $H = H_M$, yet when applied to fGn, it yields $H = H_M$-1.

## Intermittency

### Spikes

Often, scaling systems are modeled by linear stochastic processes, leading to linear exponent $\xi(q) = qH$, i.e., $K(q)$ is neglected; the processes are sometimes called "monofractal processes," the most common examples being fBm, fGn. Nonzero $K(q)$ is associated with the physical phenomenon of "spikiness" or *intermittency*: Compare the spatial spiky and temporal nonspiky series in Fig. 1a and their structure functions in Fig. 1b.

Classically, intermittency was first identified in laboratory flows as "spottiness" (Batchelor and Townsend 1949), in the atmosphere by the concentration of most of atmospheric fluxes in tiny, sparse (fractal) regions. In solid Earth geophysics, fields such as concentrations of ore are similarly sparse and scaling, a fact that notably prompted (de Wijs 1951) to independently develop a multiplicative (cascade) model for the distribution of ore. In the 1980s, de Wijs' model was rediscovered in statistical physics as the multifractal "$p$ model" (see also Agterberg 2005).

Early quantitative intermittency definitions were developed originally for fields (space). These are of the "on-off" type: When the temperature, wind, or other field exceeds a threshold, then it is "on," i.e., in a special state – perhaps of strong/violent activity. At a specific measurement resolution, the on-off intermittency can be defined as the fraction of space that the field is "on" (where it exceeds the threshold). In a scaling system, for any threshold the "on" region will be a fractal set (sparseness characterized by $c$, eq. 2) and threshold by exponent $\gamma$. The resulting function $c(\gamma)$ describes the intermittency over all scales and all intensities (thresholds) and is related to $K(q)$ as described below. In scaling time series, the same intermittency definition applies (note that other definitions are sometimes used in deterministic chaos).

Sometimes, the intermittency is obvious, but sometimes it is hidden and underestimated or overlooked; let us discuss some examples. In order to vividly display the nonclassical intermittency, it suffices to introduce a seemingly trivial tool – a "spike plot." A spike plot is the series (or transect) of the absolute first differences $\overline{\Delta f}$normalized by their means, $\Delta f / \overline{\Delta f}$ (for a series $f$). Fig. 2 shows examples from the main atmospheric scaling regimes (temperatures, the middle figure corresponds to the macroweather data analyzed in Fig. 1a, 1b). Fig. 3 shows examples from solid earth geophysics. The resolutions have been chosen to be within the corresponding scaling regimes. In Fig. 2, one immediately notices that with a single exception – macroweather in time – all of the regimes are highly "spikey," exceeding the maximum expected for Gaussian processes by a large margin (the solid horizontal line). Indeed, for the five other plots, the maxima corresponds to (Gaussian) probabilities $p < 10^{-9}$ (the top dashed line), and four of the six to $p < 10^{-20}$. The exception – macroweather in time – is the only process that is close to Gaussian behavior, but even macroweather is highly non-Gaussian in space (bottom, middle). In Fig. 3, we show corresponding examples from the KTB borehole of density and susceptibility of rocks. For the susceptibility, the intermittency is so extreme as to be noticeable in the original series (upper right), but less so for the rock density (upper left). In both cases, the spike plots (bottom row) are strongly non-Gaussian with extremes corresponding to Gaussian probabilities of $10^{-15}$, $10^{-162}$, respectively.

### Codimensions and Singularities

In order to understand the spike plots, recall that if a process is scaling, we have eq. 1 where $\varphi_{\Delta t}$ is the (normalized) flux driving the process. The normalized spikes $\Delta T / \overline{\Delta T}$ can thus be interpreted as estimates of the nondimensional, normalized driving fluxes:

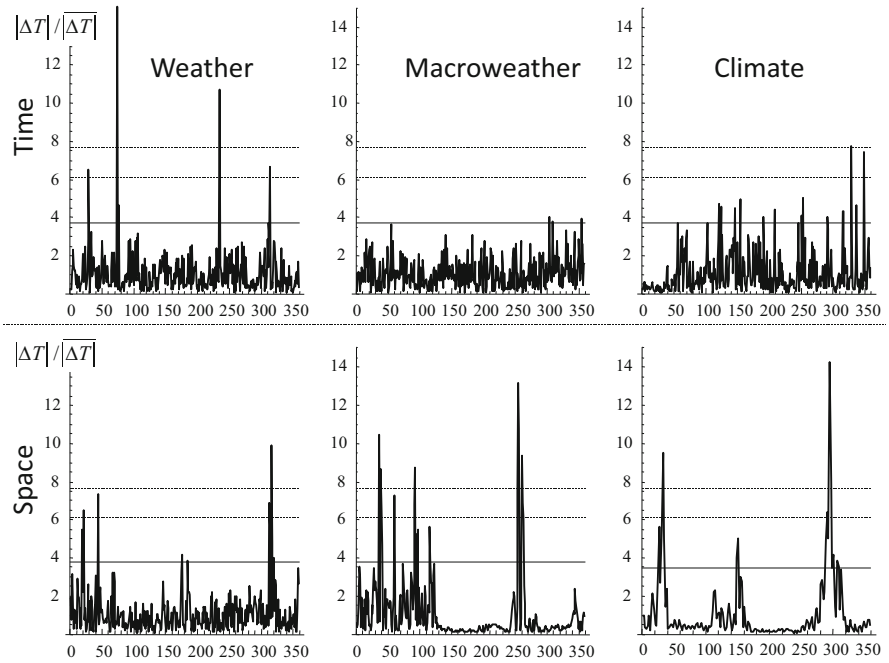


**Scaling and Scale Invariance, Fig. 2** Temperature spike plots for weather, macroweather, climate (left to right), and time and space (top and bottom rows). The solid horizontal black line indicates the expected maximum for a Gaussian process with the same number of points (360 for each with the exception of the lower right which had only 180 points); the dashed lines are the corresponding probability levels $p = 10^{-6}$, $p = 10^{-9}$ for Gaussian processes; and two of the spikes exceed 14; $p < 10^{-77}$. The upper left is Montreal at 1 hour resolution; upper middle Montreal at 4 month resolution; upper right, paleotemperatures from Greenland ice cores (GRIP) at 240 year resolution; lower left aircraft at 280 m resolution; lower middle one monthly resolution temperatures at 1o resolution in space; lower right 140 year resolution in time, 2o in space at 45oN. Reproduced from [*Lovejoy*, 2018]

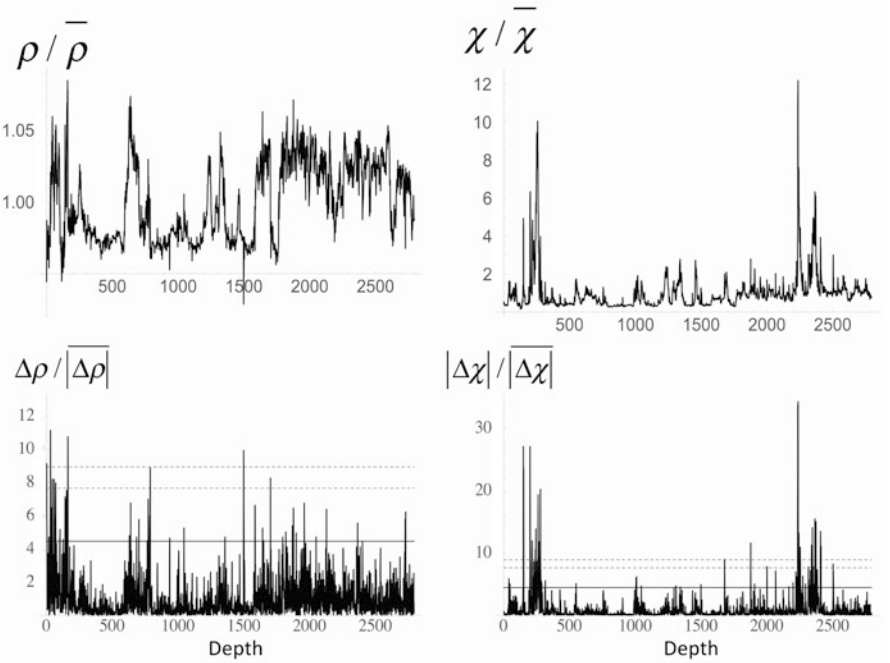


**Scaling and Scale Invariance, Fig. 3** Density (left), magnetic susceptibility (right), nondimensionalized by their means (top), and corresponding spike plots (normalized absolute first differences, bottom). The data are from the first 2795 points of the KTB borehole, each point at a 2 m interval; the horizontal axis indicates the number of points from the surface. In the spike plots, the solid line indicates the maximum expected for a Gaussian process, the dashed lines corresponding to (Gaussian) probability levels of $10^{-9}$, $10^{-12}$. The extreme spikes correspond to Gaussian probabilities of $\approx 10^{-15}$, $10^{-162}$, respectively

$$\Delta T(\Delta t)/\overline{\Delta T(\Delta t)} = \varphi_{\Delta t,un}/\overline{\varphi_{\Delta t,un}} = \varphi_{\Delta t} \tag{13}$$

(where $\varphi_{\Delta t,\ un}$ is the raw, unnormalized flux, the overbar indicates an average over the series). The interpretation in terms of fluxes comes from turbulence theory and is routinely used to quantify turbulence. In the weather regime in respectively time and space, the squares and cubes of the wind spikes are estimates of the turbulent energy fluxes. This spikiness is because most of the dynamically important events are sparse, hierarchically clustered, occurring mostly in storms and the center of storms.

The spikes visually display the intermittent nature of the process. As long as $H < 1$ (true for nearly all geo-processes), the differencing that yields the spikes acts as a high pass filter, and the spikes are dominated by the high frequencies. The Gaussian fGn, fBm processes – or nonscaling processes such as autoregressive and moving average processes (and the hybrid fractional versions of these) – will have spikes that look like the macroweather spikes: In Figs. 2 and 3, they will be roughly bounded by the (Gaussian) solid horizontal lines.

To go beyond Gaussians to the general multifractal scaling case, each spike is considered to be a singularity of order γ:

$$\lambda^{\gamma} = |\Delta f|/\overline{|\Delta f|} \tag{14}$$

λ is the scale ratio: λ = (the length of the series) / (the resolution of the series) = the number of pixels; in Fig. 3, λ = 2795. The most extreme spike ($|\Delta f|/\overline{|\Delta f|}$) therefore has a probability ≈1/2795. For Gaussian processes, spikes with this probability have $|\Delta f|/\overline{|\Delta f|} = 4.47$; this is shown by the solid lines in Fig. 3; the line therefore corresponds to $\gamma = \log\left(|\Delta f|/\overline{|\Delta f|}\right)/\log\lambda \approx \log 4.47/\log 2795 \approx 0.19$. For comparison, the actual maxima from the spike plots are $\gamma_{max} = \log(34.5)/\log(2795) = 0.45$ and $\log(11.6)/\log(2795) = 0.30$ (susceptibility, density, respectively). These values are close to those predicted by multifractal models for these processes (for more details, see Lovejoy 2018).

To understand the spike probabilities, recall that the statistics of $\varphi_\lambda$ were defined above by the moments, and $K(q)$. However, this is equivalent to specifying them via the corresponding (multiscaling) probability distributions:

$$\Pr(\varphi_\lambda > s) \approx \lambda^{-c(\gamma)}; \quad \gamma = \frac{\log s}{\log \lambda} \tag{15}$$

where "≈" indicates equality to within an unimportant prefactor and $c(\gamma)$ is the codimension function that specifies how the probabilities change with scale (Eq. 2 with $\lambda \propto L^{-1}$ and $\Pr \propto \rho$). In scaling systems, the relationship between probabilities and moments is between the corresponding scaling exponents $c(\gamma)$, $K(q)$. It turns out that it is given by the simple Legendre transformation:

$$\begin{aligned} c(\gamma) &= \max_q (q\gamma - K(q)) \\ K(q) &= \max_\gamma (q\gamma - c(\gamma)) \end{aligned} \tag{16}$$

(Parisi and Frisch 1985). The Legendre relations are generally well behaved since *K and c* are convex, although discontinuities in the first- and second-order derivatives can occur notably due to the divergence of high-order moments $q > q_D$ ("multifractal phase transitions"). The Legendre transformation also allows us to interpret $c(\gamma)$ as the fractal codimension of the set of points characterized by the singular behavior $\lambda^{\gamma}$.

Returning to the spike plots, using Eq. 15 and the estimate Eq. 14 for the singularities, we can write the probability distribution of the spikes as:

$$\Pr\left(|\Delta f|/\overline{|\Delta f|} > s\right) \approx \lambda^{-c(\gamma)}; \quad \gamma = \frac{\log s}{\log \lambda} \tag{17}$$

$\Pr\left(|\Delta f|/\overline{|\Delta f|} > s\right)$ is the probability that a randomly chosen spike $|\Delta f|/\overline{|\Delta f|}$ exceeds a fixed threshold $s$ (it is equal to one minus the more usual cumulative distribution function). $c(\gamma)$ characterizes sparseness because it quantifies how the probabilities of spikes of different amplitudes change with resolution λ (for example, when they are smoothed out by averaging). The larger $c(\gamma)$, the sparser the set of spikes that exceed the threshold $s = \lambda^{\gamma}$. A series is intermittent whenever it has spikes with $c > 0$. Gaussian series are not intermittent since $c(\gamma) = 0$ for all the spikes.

If there were no constraints on the system beyond scaling, an empirical specification would require the (unmanageable) determination of the entire scale-invariant functions $c(\gamma)$ or $K(q)$: the equivalent of an infinite number of parameters. Fortunately, it turns out that stable, attractive "universal" multifractal processes exist that require only two parameters:

$$K(q) = \frac{C_1}{(\alpha - 1)}(q^{\alpha} - q) \tag{18}$$

where $0 \le \alpha \le 2$ is the Levy index that characterizes the degree of multifractality (Schertzer and Lovejoy 1987). Notice that for any α, the intermittency parameter $C_1 = K'(1)$ and in addition $\alpha = K''(1)/K'(1)$. Together, α and $C_1$ thus characterize the tangent and curvature of $K$ near the mean ($q = 1$). For the universal multifractal probability exponent, the Legendre transformation of eq. 18 yields:

$$c(\gamma) = C_1\left(\frac{\gamma}{C_1\alpha'} + \frac{1}{\alpha}\right)^{\alpha'} \tag{19}$$

where the auxiliary variable α' is defined by: $1/\alpha' + 1/\alpha = 1$. This means that processes, whose moments have exponents $K(q)$ given by eq. 7, have probabilities with exponents $c(\gamma)$ given by eq. 15. Empirically, most geofields have α in the range 1.5–1.9, not far from the "log-normal" multifractal ($\alpha = 2$).

The $c(\gamma)$, $K(q)$ codimension multifractal formalism is appropriate for stochastic multifractals (Schertzer and Lovejoy 1987). Another commonly used multifractal formalism (often used in solid earth geophysics (Cheng and Agterberg 1996) is the dimension formalism of (Halsey et al. 1986) that was developed for characterizing phase spaces in deterministic chaos with notation $f_d(\alpha_d)$, $\alpha_d$, $\tau_d(q)$. In a finite dimensional space of dimension $d$, $f_d(\alpha_d) = d - c(\gamma)$

where $\alpha_d = d - \gamma$, and $\tau_d(q) = (q-1)d - K(q)$ where the subscript "$d$" (the dimension of the space) has been added to emphasize that unlike $c$, $\gamma$, $K$, in the dimension formalism, the basic quantities depend on both the statistics as well as $d$. For example, whereas $c$, $\gamma$, and $K$ are the same for 1-D transects, 2-D sections, or 3-D spaces, $f_d$, $\alpha_d$, and $\tau_d$ are different for each subspace.

## Scaling in Two or Higher Dimensional Spaces: Generalized Scale Invariance

### Scale Functions and Scale-Changing Operators: From Self-Similarity to Self-Affinity

If we only consider scaling in 1-D (series and transects), the notion of scale itself can be taken simply as an interval (space, $\Delta x$) or lag (time, $\Delta t$), and large scales are simply obtained from small ones by multiplying by their scale ratio $\lambda$. More general geoscience series and transects are only 1-D subspaces of ($\underline{r}$, $t$) space-time geoprocesses. In both the atmosphere and the solid earth, an obvious issue arises due to vertical/horizontal stratification: We do not expect the scaling relationship between small and large to be the same in horizontal and in vertical directions. Unsurprisingly, the corresponding transects generally have different exponents ($\xi(q)$, $H$, $K(q)$, $c(\gamma)$). In general, the degree of stratification of structures systematically changes with scale. To deal with this fundamental issue, we need an anisotropic definition of the notion of scale itself.

The simplest scaling stratification is called "self-affinity": The squashing is along orthogonal directions whose directions are the same everywhere in space, for example, along the $x$ and $z$ axes in an $x$-$z$ space, e.g., a vertical section of the atmosphere or solid earth. More generally, even horizontal sections will not be self-similar: As the scale changes, structures will be both squashed and rotated with scale. A final complication is that the anisotropy can depend not only on scale but also on position. Both cases can be dealt with by using the formalism of Generalized Scale Invariance (GSI; Schertzer and Lovejoy 1985b), corresponding respectively to linear (scale only) and nonlinear GSI (scale and position) (Lovejoy and Schertzer 2013, ch. 7; Lovejoy 2019, ch. 3).

The problem is to define the notion of scale in a system where there is no characteristic size. Often, the simplest (but usually unrealistic) "self-similar" system is simply assumed without question: The notion of scale is taken to be isotropic. In this case, it is sufficient to define the scale of a vector $\underline{r}$ by the usual vector norm (the length of the vector $\underline{r}$ denoted by $|\underline{r}| = (x^2 + z^2)^{1/2}$. $|\underline{r}|$ satisfies the following elementary scaling rule:

$$|\lambda^{-1}\underline{r}| = \lambda^{-1}|\underline{r}| \tag{20}$$

where again, $\lambda$ is a scale ratio. When $\lambda > 1$, this equation says that the scale (here, length) of the reduced, shrunken vector $\lambda^{-1}\underline{r}$ is simply reduced by the factor $\lambda^{-1}$, a statement that holds for any orientation of $\underline{r}$.

To generalize this, we introduce a more general scale function $\|\underline{r}\|$ as well as a more general scale-changing operator $T_\lambda$; together they satisfy the analogous equation:

$$\|T_\lambda \underline{r}\| = \lambda^{-1}\|\underline{r}\| \tag{21}$$

For the system to be scaling, a reduction by scale ratio $\lambda_1$ followed by a reduction $\lambda_2$ should be equal to first reduction by $\lambda_2$ and then by $\lambda_1$, and both should be equivalent to a single reduction by factor $\lambda = \lambda_1 \lambda_2$. The scale-changing operator therefore satisfies group properties, so $T_\lambda$ is a one-parameter Lie group with generator $G$:

$$T_\lambda = \lambda^{-G} \tag{22}$$

When $G$ is the identity operator ($I$), then $T_\lambda \underline{r} = \lambda^{-I}\underline{r} = \lambda^{-1} I \underline{r} = \lambda^{-1}\underline{r}$ so that the scale reduction is the same in all directions (an isotropic reduction): $\|\lambda^{-1}\underline{r}\| = \lambda^{-1}\|\underline{r}\|$. However, a scale function that is symmetric with respect to such isotropic changes is not necessarily equal to the usual norm $|\underline{r}|$ since the vectors with unit scale (i.e., those that satisfy $\|\underline{r}\| = 1$) may be any (nonconstant, hence anisotropic) function of the polar angle – they are not necessarily circles (2D) or spheres (3D). Indeed, in order to complete the scale function definition, we must specify all the vectors whose scale is unity – the "unit ball." If in addition to $G = I$, the unit scale is a circle (sphere), then the two conditions imply

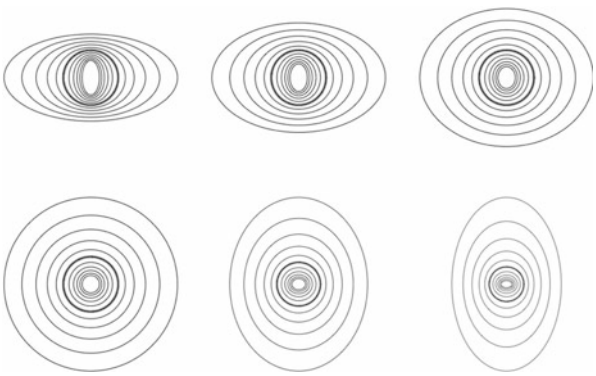

**Scaling and Scale Invariance, Fig. 4** A series of ellipses each separated by a factor of 1.26 in scale, red indicating the unit scale (here, a circle, thick lines). Upper left to lower right, $H_z$ increasing from 2/5, 3/5, 4/5 (top), 1, 6/5, 7/5 (bottom, left to right). Note that when $H_z > 1$, the stratification at large scales is in the vertical rather than the horizontal direction (this is required for modeling the earth's geological strata). Reproduced from Lovejoy (2019)

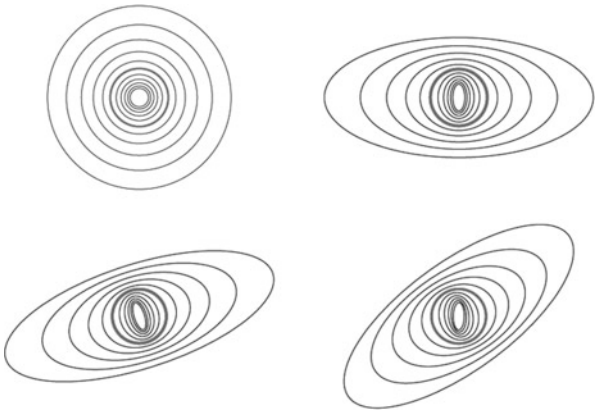

**Scaling and Scale Invariance, Fig. 5** Blowups and reductions by factors of 1.26 starting at circles (thick lines). The upper left shows the isotropic case, the upper right shows the self-affine (pure stratification case), the lower left example is stratified but along oblique directions, and the lower right example has structures that rotate continuously with scale while becoming increasingly stratified. The matrices used are: $\begin{pmatrix} 1 & 0 \\ 0 & 1 \end{pmatrix}$, $\begin{pmatrix} 1.35 & 0 \\ 0 & 0.65 \end{pmatrix}$, $\begin{pmatrix} 1.35 & 0.25 \\ 0.25 & 0.65 \end{pmatrix}$, and $\begin{pmatrix} 1.35 & -0.45 \\ 0.85 & 0.65 \end{pmatrix}$ (upper left to lower right). Reproduced from Lovejoy (2019)

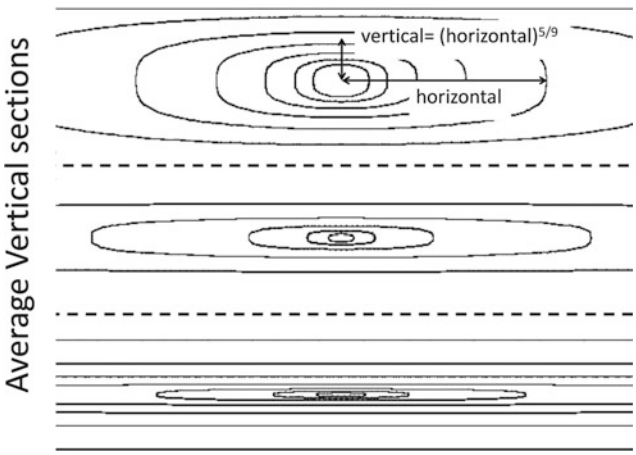


**Scaling and Scale Invariance, Fig. 6a** The theoretical shapes of average vertical cross sections using the empirical parameters estimated from CloudSat – derived mean parameters: $H_z = 5/9$, with sphero-scales 1 km (top), 100 m (middle), 10 m (bottom), roughly corresponding to the geometric mean and one-standard-deviation fluctuations. In each of the three, the distance from left to right horizontally is 100 km, from top to bottom vertically is 20 km. It uses the canonical scale function. The top figure in particular shows that structures 100 km wide will be about 10 km thick whenever the sphero-scale is somewhat larger than average (Lovejoy et al. 2009)

$\|\underline{r}\| = |\underline{r}|$ and we recover Eq. 20. In the more general – but still linear case where $G$ is a linear operator (a matrix) – $T_\lambda$ depends on scale but is independent of location; more generally – nonlinear GSI – $G$ also depends on location and scale; Figs. 4, 5, 6a, 6b and 7 give some examples of scale functions, and Figs. 8a, 8b, 9 and 10 show some of the corresponding multifractal cloud, magnetization, and topography simulations.

## Scaling Stratification in the Earth and Atmosphere

GSI is exploited in modeling and analyzing the earth's density and magnetic susceptibility fields (the review Lovejoy and Schertzer 2007), and in many atmospheric fields (wind, temperature, humidity, precipitation, cloud density, and aerosol concentrations; see the monograph Lovejoy and Schertzer 2013). To give the idea, we can define the "canonical" scale function for the simplest stratified system representing a vertical $(x,z)$ section in the atmosphere or solid earth:

$$\|(x,z)\| = l_s \left| \left(\frac{x}{l_s}\right), sign(z)\left|\frac{z}{l_s}\right|^{1/H_z} \right| = l_s \left[ \left(\frac{x}{l_s}\right)^2 + \left|\frac{z}{l_s}\right|^{2/H_z} \right]^{1/2} \quad (23)$$

$H_z$ characterizes the degree of stratification (see below), and $l_s$ is the "sphero-scale," so-called because it defines the scale at which horizontal and vertical extents of structures are equal (although they are generally not exactly circular):

$$\|(l_s,0)\| = \|(0,l_s)\| = l_s \quad (24)$$

It can be seen by inspection that $\|(x, z)\|$satisfies:

$$\|T_\lambda(x,z)\| = \lambda^{-1}\|(x,z)\|; \quad T_\lambda = \lambda^{-G}; \quad G = \begin{pmatrix} 1 & 0 \\ 0 & H_z \end{pmatrix} \quad (25)$$

(note that matrix exponentiation is simple only for diagonal matrices – here $T_\lambda = \begin{pmatrix} \lambda^{-1} & 0 \\ 0 & \lambda^{-H_z} \end{pmatrix}$ – but when $G$ is not diagonal, it can be calculated by expanding the series: $\lambda^{-G} =$

**Scaling and Scale Invariance, Fig. 6b** Vertical cross-section of the magnetization scale function assuming $H_z = 2$ and a sphero-scale of 40,000 km. The scale is in kilometers and the aspect ratio is ¼ (Lovejoy et al. 2001)

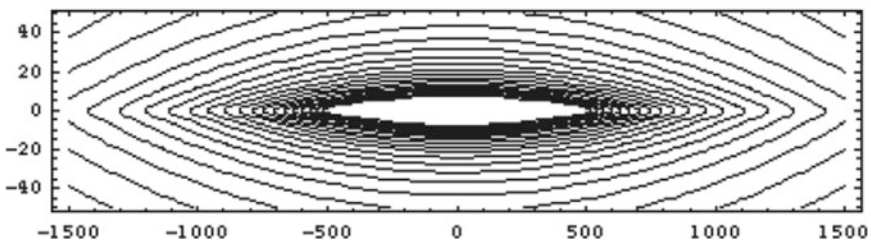

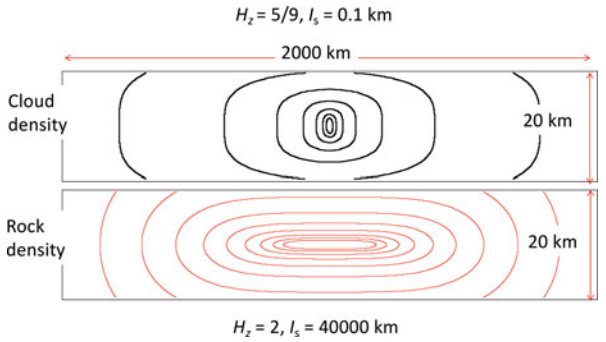


**Scaling and Scale Invariance, Fig. 7** The unity of geoscience illustrated via a comparison of typical (average) vertical sections in the atmosphere (top), and in the solid earth (bottom), an aspect ratio of 1/5 was used. The key points are as follows: $H_z < 1$, $l_s$ small (atmosphere, stratification increasing at larger scales) and $H_z > 1$, $l_s$ large (solid earth, stratification increasing at smaller scales). The sphero-scale ($l_s$) varies in space and in time (see Fig. 6a, 6b)

$e^{-G \log \lambda} = 1 - G \log \lambda + (G \log \lambda)^2/2 - \ldots$). Notice that in this case, the ratios of the horizontal/vertical statistical exponents (i.e., $\xi(q)$, $H$, $K(q)$, and $c(\gamma)$) are equal to $H_z$. We could also note that linear transects taken any direction other than horizontal or vertical will have two scaling regimes (with a break near the sphero-scale). However, the break is spurious; it is a consequence of using the wrong notion of scale.

Equipped with a scale function, the general anisotropic generalization of the 1-D scaling law (Eq. 1) may now be expressed by using the scale $\|\underline{\Delta r}\|$:

$$\Delta f(\underline{\Delta r}) \stackrel{d}{=} \varphi_{\|\underline{\Delta r}\|} \|\underline{\Delta r}\|^H \tag{26}$$

This shows that the full scaling model or full characterization of scaling requires the specification of the notion of scale via the scale-invariant generator $G$ and unit ball (hence the scale function), the fluctuation exponent $H$, as well the statistics of $\varphi_{\|\underline{\Delta r}\|}$ specified via $K(q)$, $c(\gamma)$ or – for universal multifractals, $C_1$, $\alpha$. In many practical cases – e.g., vertical stratification – the direction of the anisotropy is fairly obvious, but in horizontal sections, where there can easily be significant rotation of structures with scale, the empirical determination of $G$ and the scale function is a difficult, generally unsolved problem.

In the atmosphere, it appears that the dynamics are dominated by Kolmogorov scaling in the horizontal ($H_h = 1/3$) and Bolgiano-Obhukhov scaling in the vertical ($H_v = 3/5$) so that $H_z = H_h/H_v = 5/9 = 0.555...$ Assuming that the horizontal directions have the same scaling, then typical structures of size $L$x$L$ in the horizontal have vertical extents of $L^{Hz}$, hence their volumes are $L^{Del}$ with "elliptical dimension" $D_{el} = 2 + H_z = 2.555\ldots$; the "23/9D model" (Schertzer and Lovejoy 1985a). This model is very close to the empirical data, and it contradicts the "standard model" that is based on isotropic symmetries and that attempts to combine a small-scale isotropic 3D regime and a large-scale isotropic (flat) 2D regime with a transition supposedly near the atmospheric scale height of 10 km. The requisite transition has never been observed, and claims of large-scale 2D "geostrophic" turbulence have been shown to be spurious (reviewed in ch. 2 of Lovejoy and Schertzer 2013).

Since $H_z < 1$, the atmosphere becomes increasingly stratified at large scales. In solid earth applications, it was found that $H_z \approx 2$–3 (rock density, susceptibility, and hydraulic conductivity (Lovejoy and Schertzer 2007)) i.e., $H_z > 1$ implying on the contrary that the earth's strata are typically more horizontally stratified at the smallest scales (Figs. 6a, 6b and 7).

## Conclusions

Geosystems typically involve structures spanning wide ranges of scale: from the size of the planet down to millimetric dissipations scales (the atmosphere) or micrometric scales (solid earth). Classical approaches stem from the outdated belief that complex behavior requires complicated models. The result is a complicated "scalebound" paradigm involving hierarchies of phenomenological models / mechanisms each spanning small ranges of scale. For example, conventionally, the atmosphere was already divided into synoptic, meso- and microscales when Orlanski (1975) proposed further divisions implying new mechanisms every factor of two or so in scale. Ironically, this still popular paradigm arose at the same time that scale-free numerical weather and climate models were being developed that were based on the scaling dynamical equations and now known to display scaling meteorological fields.

At the same time as the scale-bound paradigm was ossifying, the "Fractal Geometry of Nature" (Mandelbrot 1977, 1982) proposed an opposite approach based on sets that respected an isotropic scaling symmetry: self-similar fractals. These have scale-free power law number-size relationships whose exponents are scale-invariant geo-applications already included topography and clouds. However, geosystems are rarely geometric sets of points but rather fields (i.e., with values, e.g., temperature, rock density) varying in space and in time. In addition, these fields are typically highly anisotropic notably with highly stratified vertical sections. In the 1980s, the necessary generalizations to scaling fields (multifractals) and to anisotropic scaling (Generalized Scale Invariance, GSI) were achieved.

GSI clarifies the significance of scaling in geoscience since it shows that scaling is a rather general symmetry principle: It is thus the simplest relation between scales. Just as the classical symmetries (temporal, spatial invariance, and directional invariance) are equivalent (Noether's theorem) to

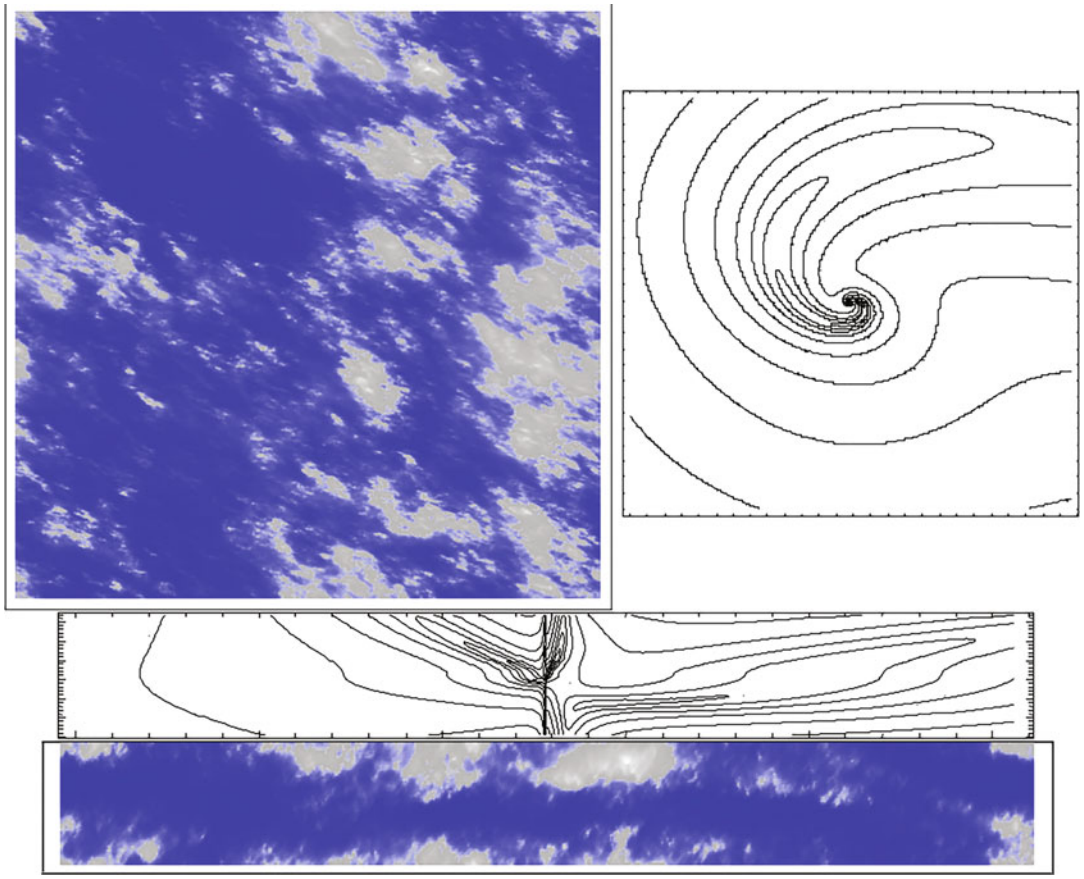

**Scaling and Scale Invariance, Fig. 8a** Simulations of the liquid water density field. The top is a horizontal section, to the right the corresponding central horizontal cross section of the scale function. The stratification is determined by $H_z = 0.555$ with $l_s = 32$. The bottom shows side views. There is also horizontal anisotropy with rotation. Statistical (multifractal) parameters: $\alpha = 1.8$, $C_1 = 0.1$, and $H = 0.333$, on a 512x512x64 grid (Lovejoy and Schertzer 2013)

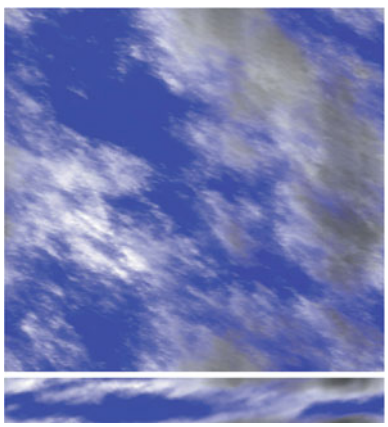

**Scaling and Scale Invariance, Fig. 8b** The top is the visible radiation field (corresponding to Fig. 8a), looking up (sun at 45° from the right); the bottom is a side radiation field (one of the 512x64 pixel sides) (Lovejoy and Schertzer 2013)

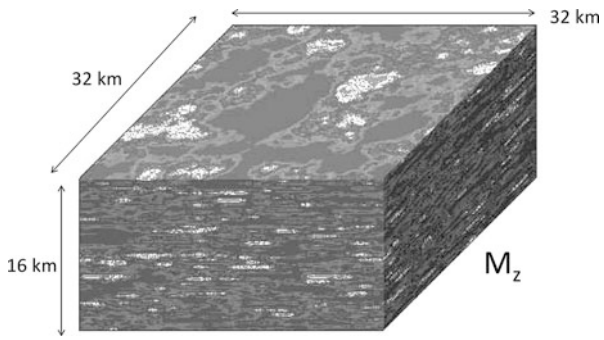


**Scaling and Scale Invariance, Fig. 9** Numerical simulation of a multifractal rock magnetization field (vertical, component $M_z$) with parameters deduced from rock samples and near surface magnetic anomalies (Pecknold et al. 2001). The simulation was horizontally isotropic with vertical stratification specified by $H_z = 1.7$, $l_s = 2500$ km; the region is 32x32x16 km, resolution 0.25 km. The statistical parameters specifying the horizontal multifractal statistics are $H = 0.2$, $\alpha = 1.98$, and $C_1 = 0.08$. This is a reasonably realistic crustal section, although the spheroscale was taken to be a bit too small in order that strata may be easily visible. Notice that the structures become more stratified at smaller scales. The direction of M is assumed to be fixed in the z direction

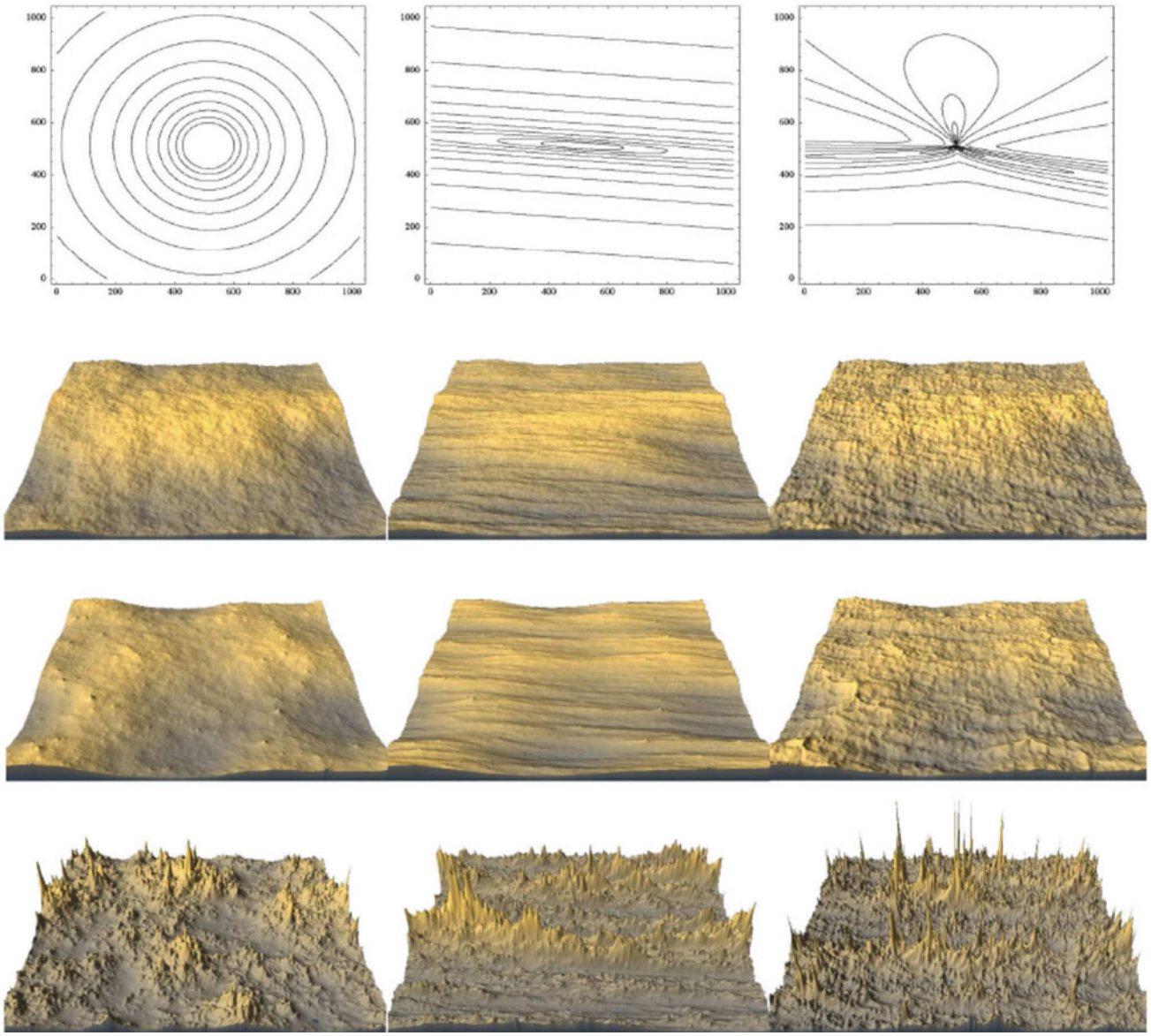

**Scaling and Scale Invariance, Fig. 10** Comparison of isotropic versus anisotropic simulations for three different scaling models. Top row shows the scale functions. From left to right, we change the type of anisotropy: The left column is self-similar (isotropic) while the middle and right columns are anisotropic and symmetric with respect to $G = \begin{pmatrix} 0.8 & -0.5 \\ 0.05 & 1.2 \end{pmatrix}$. The middle column has unit ball circular at 1 pixel, while for the right one the unit ball is also anisotropic. The second, third, and fourth rows show the corresponding fBm (with $H = 0.7$), the analogous fractional Levy motion (fLm $\alpha = 1.8$, $H = 0.7$), and multifractal ($\alpha = 1.8$, $C1 = 0.12$, $H = 0.7$) simulations. We note that in the case of fBm, one mainly perceives textures; there are no very extreme mountains or other morphologies evident. One can see that the fLm is too extreme; the shape of the singularity (particularly visible in the far right) is quite visible in the highest mountain shapes. The multifractal simulations are more realistic in that there is a more subtle hierarchy of mountains. When the contour lines of the scale functions are close, the scale $\|\underline{r}\|$ changes rapidly over short distances. For a given order of singularity $\gamma$, $\lambda^{\gamma}$ will therefore be larger. This explains the strong variability depending on direction (middle bottom row) and on shape of unit ball (right bottom row). Indeed, spectral exponents will be different along the different eigenvectors of $G$ (Lovejoy and Schertzer 2007).

conservation laws (energy, momentum, and angular momentum), the (nonclassical) scaling symmetry conserves the scaling functions $G$, $K$, and $c$. Symmetries are fundamental since they embody the simplest possible assumption, model: Under a system change, there is an invariant. In physics, initial assumptions about a system are that it respects symmetries. Symmetry breaking is only introduced on the basis of strong evidence or theoretical justification: in the case of scale symmetries, they are broken by the introduction. of characteristic space or time scales.

Theoretically, scaling is a unifying geophysical principle that has already shown its realism in numerous geoapplications both on Earth and Mars proving the pertinence of anisotropic scaling models and analyses. It is unfortunate that in geoscience, scale-bound models and analyses continue to be justified on superficial phenomenological grounds. Geoapplications of scaling are therefore still in their infancy.

## References


Agterberg F (2005) New applications of the model of de Wisj in regional geochemistry. Math Geol. https://doi.org/10.1007/s11004-006-96063-7

Batchelor GK, Townsend AA (1949) The nature of turbulent motion at large wavenumbers. Proc R Soc Lond A 199:238

Chen W, Lovejoy S, Muller JP (2016) Mars' atmosphere: the sister planet, our statistical twin. J Geophys Res Atmos 121. https://doi.org/10.1002/2016JD025211

Cheng Q, Agterberg F (1996) Multifractal modelling and spatial statistics. Math Geol 28:1–16

de Wijs HJ (1951) Statistics of ore distribution, part I. Geol Mijnb 13: 365–375

Feller W (1971) An introduction to probability theory and its applications, vol 2. Wiley, p 669

Grassberger P, Procaccia I (1983) Measuring the strangeness of strange atractors. Physica 9D:189–208

Halsey TC, Jensen MH, Kadanoff LP, Procaccia I, Shraiman B (1986) Fractal measures and their singularities: the characterization of strange sets. Phys Rev A 33:1141–1151

Hentschel HGE, Procaccia I (1983) The infinite number of generalized dimensions of fractals and strange attractors. Physica D 8:435–444

Hooge C, Lovejoy S, Pecknold S, Malouin JF, Schertzer D (1994) Universal multifractals in seismicity. Fractals 2:445–449

Hurst HE (1951) Long-term storage capacity of reservoirs. Trans Am Soc Civ Eng 116:770–808

Kolmogorov AN (1940) Wienershe spiralen und einige andere interessante kurven in Hilbertschen Raum. Doklady Academii Nauk SSSR 26:115–118

Lamperti J (1962) Semi-stable stochastic processes. Trans Am Math Soc 104:62–78

Landais F, Schmidt F, Lovejoy S (2019) Topography of (exo)planets. MNRAS 484:787–793. https://doi.org/10.1093/mnras/sty3253

Lovejoy S (2018) The spectra, intermittency and extremes of weather, macroweather and climate. Nat Sci Rep 8:1–13. https://doi.org/10.1038/s41598-018-30829-4

Lovejoy S (2019) *Weather, macroweather and climate: our random yet predictable atmosphere*. Oxford University Press, p 334

Lovejoy S, Schertzer D (2007) Scaling and multifractal fields in the solid earth and topography. Nonlin Processes Geophys 14:1–38

Lovejoy S, Schertzer D (2012) Haar wavelets, fluctuations and structure functions: convenient choices for geophysics. Nonlinear Proc Geophys 19:1–14. https://doi.org/10.5194/npg-19-1-2012

Lovejoy S, Schertzer D (2013) *The weather and climate: emergent Laws and Multifractal cascades*, 496 pp. Cambridge University Press

Lovejoy S, Schertzer D, Ladoy P (1986) Fractal characterisation of inhomogeneous measuring networks. Nature 319:43–44

Lovejoy S, Pecknold S, Schertzer D (2001) Stratified multifractal magnetization and surface geomagnetic fields, part 1: spectral analysis and modelling. Geophys J Inter 145:112–126

Lovejoy S, Pinel J, Schertzer D (2012) The global space-time Cascade structure of precipitation: satellites, gridded gauges and reanalyses. Adv Water Resour 45:37–50. https://doi.org/10.1016/j.advwatres.2012.03.024

Lovejoy S, Tuck AF, Schertzer D, Hovde SJ (2009) Reinterpreting aircraft measurements in anisotropic scaling turbulence. Atmos Chem Phys 9: 1–19.

Mandelbrot BB (1977) Fractals, form, chance and dimension. Freeman

Mandelbrot BB (1982) The fractal geometry of nature. Freeman

Mandelbrot BB, Van Ness JW (1968) Fractional Brownian motions, fractional noises and applications. SIAM Rev 10:422–450

Marsan D, Schertzer D, Lovejoy S (1996) Causal space-time multifractal processes: predictability and forecasting of rain fields. J Geophy Res 31D:26333–326346

Orlanski I (1975) A rational subdivision of scales for atmospheric processes. Bull Amer Met Soc 56:527–530

Parisi G, Frisch U (1985) A multifractal model of intermittency. In: Ghil M, Benzi R, Parisi G (eds) Turbulence and predictability in geophysical fluid dynamics and climate dynamics. North Holland, pp 84–88

Pecknold S, Lovejoy S, Schertzer D (2001) Stratified multifractal magnetization and surface geomagnetic fields, part 2: multifractal analysis and simulation. Geophys Inter J 145:127–144

Schertzer D, Lovejoy S (1983) On the dimension of atmospheric motions, paper presented at IUTAM Symp. In: On turbulence and chaotic phenomena in fluids, Kyoto, Japan

Schertzer D, Lovejoy S (1985a) The dimension and intermittency of atmospheric dynamics. In: Bradbury LJS, Durst F, Launder BE, Schmidt FW, Whitelaw JH (eds) *Turbulent shear flow*. Springer-Verlag, pp 7–33

Schertzer D, Lovejoy S (1985b) Generalised scale invariance in turbulent phenomena. Physico-Chemical Hydrodynamics Journal 6: 623–635

Schertzer D, Lovejoy S (1987) Physical modeling and analysis of rain and clouds by anisotropic scaling of multiplicative processes. J Geophys Res 92:9693–9714

Taleb NN (2010) *The Black Swan: the impact of the highly improbable*. Random House, p 437pp